

---

# CoRDE: Concept-Prior Routed Diffusion Experts for Structural Generalization in Robot Manipulation

---

Anonymous Author(s)

Affiliation

Address

email

## Abstract

1 Diffusion models excel at capturing multi-modal action distributions in robot im-  
2 itation learning. However, in multi-task and long-horizon scenarios, monolithic  
3 architectures lack structural generalization capabilities, suffering from gradient  
4 conflicts between distinct semantic sub-stages. While pure data-driven Mixture-of-  
5 Experts (MoE) methods introduce labor division, they frequently trigger routing  
6 collapse, and instantiating full-scale experts causes parameter explosion and high  
7 expansion costs. To address these issues, we propose Concept-prior Routed Dif-  
8 fusion Experts (CoRDE), a structure-guided variational distillation framework.  
9 CoRDE extracts semantic distributions from a frozen concept encoder to guide  
10 the variational posterior responsibility via a learnable soft mapping matrix. This  
11 mechanism enforces a dual-entropy dynamics conservation: it minimizes routing  
12 entropy to guarantee macroscopic cognitive certainty, while preserving the full-  
13 rank variance of the stochastic diffusion term to maintain behavioral diversity. To  
14 overcome parameter inflation, CoRDE employs a parameter-efficient expert pool  
15 using Low-Rank Adaptation (LoRA) on a shared frozen backbone. Rigorous math-  
16 ematical proofs demonstrate that the mixture score field of low-rank experts strictly  
17 approximates the teacher distribution in the least-squares sense, avoiding rank-  
18 deficiency-induced diversity loss and ensuring high-fidelity generation. Empirical  
19 evaluations confirm that, compared to existing baselines, CoRDE systematically  
20 reduces routing collapse, forming robust, semantically aligned expert allocations  
21 while achieving superior action quality and incremental learning efficiency.

## 22 1 INTRODUCTION

23 It is well established that diffusion models, which formulate action generation as a conditional  
24 denoising process, have become a dominant paradigm in robot imitation learning [2, 3, 14, 16].  
25 By learning the score function within the action space, diffusion policies excel at capturing highly  
26 complex, multi-modal, and continuous data distributions inherent in human demonstrations. This  
27 expressive capability allows robots to replicate diverse human behaviors with unprecedented trajectory  
28 smoothness and high task success rates. Despite these significant advances, deploying monolithic  
29 diffusion policies in multi-task and long-horizon scenarios reveals severe structural limitations.  
30 Forcing a single set of global parameters to simultaneously represent behavioral modes with drastically  
31 heterogeneous frequency properties inevitably induces gradient conflicts [4, 7, 11, 8] and catastrophic  
32 interference. Furthermore, their iterative denoising nature incurs substantial inference latency, while  
33 intractable likelihoods complicate post-hoc policy optimization.

34 To mitigate these bottlenecks, recent research transforms pre-trained diffusion policies into Mixture of  
35 Experts (MoE) architectures [15, 18, 10], notably via Variational Distillation of Diffusion (VDD) [22].  
36 Simultaneously, other expert-driven manipulation frameworks [5, 20] have been utilized to decompose  
37 manipulation skills. However, existing unsupervised MoE frameworks [22, 20, 17] are constrained  
38 by fundamental contradictions: when processing noisy multi-modal data, pure data-likelihood-driven

39 routing frequently triggers routing collapse [22] and distorts the naturally uneven distribution of  
 40 physical tasks [17]. Additionally, the resulting expert populations lack human-interpretable semantic  
 41 boundaries, and instantiating full-scale experts causes parameter explosion.

42 In this article, we present Concept-prior Routed Diffusion Experts (CoRDE), a novel structure-guided  
 43 variational distillation system that seamlessly unifies high-level semantic concept priors [23, 13]  
 44 with the generative expressivity of diffusion MoE models. Our approach extracts a stable semantic  
 45 distribution from a frozen concept encoder to guide the variational posterior responsibility via a  
 46 learnable soft mapping matrix. This enforces a dual-entropy dynamics conservation: minimizing  
 47 routing entropy for macroscopic certainty, while preserving the full-rank variance of the stochastic  
 48 diffusion term [19] to maintain behavioral diversity. To overcome parameter inflation, we construct an  
 49 expert pool by injecting Low-Rank Adaptation (LoRA) [6] modules onto a shared frozen backbone.  
 50 We provide rigorous mathematical proofs demonstrating that the mixture score field of low-rank  
 51 experts strictly approximates the teacher distribution in the  $L_2$  sense [22], theoretically guaranteeing  
 52 high-fidelity generation while avoiding rank-deficiency-induced diversity loss [1, 21].

53 The purpose of this article is to solve the structural generalization challenge in multi-modal robot  
 54 manipulation. Our main contributions are as follows:

- 55 • We propose a structure-guided variational diffusion distillation framework that integrates a concept-  
 56 prior-driven responsibility mechanism, systematically eliminating routing collapse and forming  
 57 robust, semantically aligned expert allocations.
- 58 • We design a parameter-efficient diffusion expert pool utilizing LoRA. Rigorous mathematical proofs  
 59 guarantee that this architecture drastically reduces computational overhead while maintaining action  
 60 diversity via the stochastic diffusion term and ensuring high-fidelity generation through strict score  
 61 field approximation.
- 62 • We develop an Expectation-Maximization (EM) style self-organizing soft alignment algorithm,  
 63 establishing an interpretable many-to-many mapping between macroscopic task concepts and  
 64 microscopic execution experts.

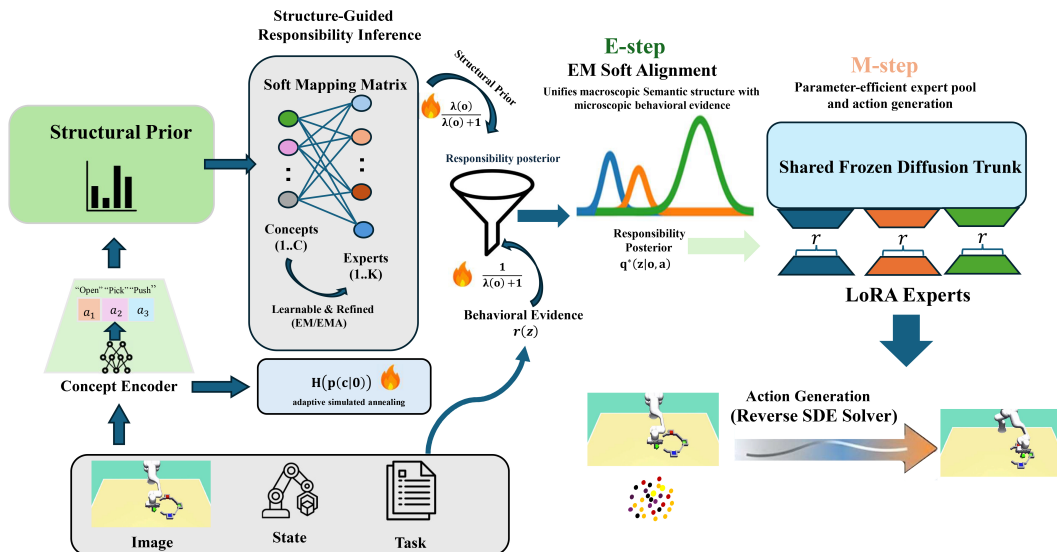


Figure 1: Overview of the CoRDE framework. **Training:** A structural prior—derived from extracted concept semantics—fuses with behavioral evidence to infer a variational responsibility posterior. This guides task allocation across parameter-efficient LoRA experts on a shared backbone. **Inference:** State-conditioned routing dynamically activates these experts. The resulting mixture score field synthesizes high-fidelity actions while strictly preserving full-rank behavioral diversity.

## 65 2 Methodology

66 This section formulates the Concept-prior Routed Diffusion Experts (CoRDE) framework. We first  
 67 establish the variational distillation of monolithic diffusion policies into a Mixture-of-Experts (MoE)  
 68 architecture. Subsequently, we construct the structure-guided responsibility inference mechanism,

69 present the parameter-efficient expert parameterization with rigorous error bounds, and detail the  
 70 self-organizing alignment updates.

## 71 2.1 Preliminaries: Distilling a Diffusion Policy into MoE

72 Diffusion policies model action generation as a conditional denoising process. Given a demonstration  
 73 dataset  $\mathcal{D} = \{(o_i, a_{0,i})\}$ , the forward process injects Gaussian noise  $\epsilon \sim \mathcal{N}(0, I)$  into the clean  
 74 action sequence  $a_0$  at continuous timestep  $t \in (0, T]$ , yielding the noisy action  $a_t = \alpha_t a_0 + \sigma_t \epsilon$ .  
 75 The monolithic diffusion policy is trained to predict the injected noise via the score-matching proxy  
 76 objective [2]:

$$\mathcal{L}_{\text{diff}} = \mathbb{E}_{o, a_0, t, \epsilon} [\|\epsilon - \epsilon_\theta(a_t, o, t)\|_2^2], \quad (1)$$

77 where  $\epsilon_T$  denotes the pre-trained teacher noise predictor. This objective is mathematically equivalent  
 78 to matching the true score field of the data distribution, i.e.,  $u_T(a_t, o, t) = -\epsilon_T(a_t, o, t)/\sigma_t \approx$   
 79  $\nabla_{a_t} \log p_t(a_t|o)$ . For strict theoretical coherence, subsequent derivations utilize the score field  
 80 notation  $u$ .

81 To overcome the intractable likelihood and elevated inference latency of diffusion models, the  
 82 Variational Distillation of Diffusion (VDD) method [22] compresses the pre-trained continuous  
 83 teacher into a single-step MoE student policy:

$$q_\phi(a|o) = \sum_{z=1}^K q_\psi(z|o) \pi_\theta(a|o, z), \quad (2)$$

84 where  $z \in \{1, \dots, K\}$  indexes the experts, and  $q_\psi(z|o)$  designates the gating network. VDD  
 85 optimizes a decompositional variational upper bound, allowing individual experts to be trained  
 86 independently. However, unsupervised MoE routing driven exclusively by data likelihood persistently  
 87 induces routing collapse or mode-averaging [17, 22]. This systemic instability motivates the  
 88 integration of macroscopic structural priors to regularize the underlying routing dynamics.

## 89 2.2 Structure-Guided Responsibility Inference and Entropy Dynamics

90 To systematically eliminate routing collapse, CoRDE imposes cognitive certainty by guiding expert  
 91 assignments with high-level semantics. Following representation paradigms like HiMaCon [13],  
 92 we deploy a frozen concept encoder to obtain the distribution  $p_\phi(c|o)$  over  $C$  semantic clusters. To  
 93 facilitate a many-to-many labor division where the expert count  $K$  operates independently of  $C$ , we  
 94 formulate the structural prior using the soft mapping matrix  $P_{CE}(z|c)$ :

$$p_{\text{struct}}(z|o) = \sum_{c=1}^C p_\phi(c|o) P_{CE}(z|c). \quad (3)$$

95 Concurrently, the behavioral evidence  $r(z|o, a_0)$  quantifies the local score-fitting precision of expert  $z$ ,  
 96 defined as  $r(z|o, a_0) = q_\psi(z|o) \exp(-\|u_T - u_\theta^{(z)}\|_2^2)$ . Let  $\bar{r}(z|o, a_0)$  denote the normalized evidence.  
 97 To unify the macroscopic semantic structure and microscopic behavioral evidence, we construct a  
 98 structure-regularized variational objective:

$$\min_{\tilde{q}} \mathbb{E}_{o, a_0} [\text{KL}(\tilde{q}||\bar{r}) + \lambda(o) \text{KL}(\tilde{q}||p_{\text{struct}})], \quad (4)$$

99 where  $\lambda(o) \geq 0$  controls the structural guidance strength.

100 *Proof of Optimal Posterior:* We formulate the Lagrangian of Eq. (4) subject to the constraint  
 101  $\sum_z \tilde{q}(z) = 1$ :

$$\begin{aligned} \mathcal{L}(\tilde{q}, \nu) &= \sum_z \tilde{q}(z) \ln \frac{\tilde{q}(z)}{\bar{r}(z|o, a_0)} + \lambda(o) \sum_z \tilde{q}(z) \ln \frac{\tilde{q}(z)}{p_{\text{struct}}(z)} \\ &\quad + \nu \left( \sum_z \tilde{q}(z) - 1 \right). \end{aligned}$$

102 Setting the partial derivative  $\frac{\partial \mathcal{L}}{\partial \tilde{q}(z)} = 0$  yields:

$$(1 + \lambda(o)) \ln \tilde{q}(z) = \ln \bar{r}(z|o, a_0) + \lambda(o) \ln p_{\text{struct}}(z) - (1 + \lambda(o) + \nu).$$

103 Solving for  $\tilde{q}(z)$  yields the optimal variational responsibility posterior  $q^*(z|o, a_0)$  as an exact geo-  
 104 metric mean:

$$q^*(z|o, a_0) = \frac{1}{Z(o, a_0)} \bar{r}(z|o, a_0)^{\frac{1}{1+\lambda(o)}} p_{\text{struct}}(z|o)^{\frac{\lambda(o)}{1+\lambda(o)}}, \quad (5)$$

105 where  $Z(o, a_0)$  is the partition function.

106 The parameter  $\lambda(o)$  anneals adaptively based on the normalized concept confidence  $\gamma(o) = 1 -$   
 107  $H(p_\phi(c|o))/\log C$ . Assigning  $\lambda(o) = \lambda_{\max}\gamma(o)$  guarantees robust fallback to evidence-driven  
 108 allocation under ambiguous semantic states.

109 **Theorem 1 (Routing Entropy Bound):** As the structural guidance strength approaches infinity  
 110 ( $\lambda(o) \rightarrow \infty$ ), the entropy of the responsibility posterior mathematically binds to the structure prior:  
 111  $\lim_{\lambda \rightarrow \infty} H(q^*) = H(p_{\text{struct}})$ . Since  $p_{\text{struct}}$  originates from a discriminative encoder characterized by  
 112 intrinsically low entropy, this fusion strictly minimizes *routing entropy*.

### 113 2.3 Parameter-Efficient LoRA Experts and $L_2$ Score Approximation

114 Instantiating full-scale diffusion networks for individual experts inflates parameters prohibitively.  
 115 Therefore, the student policy shares a frozen diffusion transformer trunk  $h_\eta(o)$ . Expert differentiation  
 116 relies solely on Attention-LoRA modules injected into the linear projection layers. For expert  $z$ , the  
 117 weight is parameterized as  $W^{(z)} = W_0 + B^{(z)}A^{(z)}$ , subject to the rank constraint  $r \ll d$ .

118 During the M-step, each expert minimizes the responsibility-weighted score-matching discrepancy  
 119 against the teacher score  $u_T$ :

$$\mathcal{L}_{\text{expert}}(z) = \mathbb{E}_{o, a_0, t, \epsilon} [\cdot] \quad (6)$$

120 **Theorem 2 (Mixture  $L_2$  Score Approximation):** Let  $\tilde{u}(a_t, o, t) \triangleq \sum_{z=1}^K q^*(z|o, a_0) u_\theta^{(z)}(a_t, o, t)$   
 121 denote the combined score field of the student experts. Utilizing Jensen’s inequality regarding the  
 122 strict convexity of the squared  $L_2$  norm (i.e.,  $\|\sum w_i x_i\|^2 \leq \sum w_i \|x_i\|^2$  for  $\sum w_i = 1$ ), the global  
 123 score discrepancy is bounded by the weighted sum of local expert errors:

$$\|u_T - \tilde{u}\|_2^2 = \left\| \sum_{z=1}^K q^*(z) (u_T - u_\theta^{(z)}) \right\|_2^2 \leq \sum_{z=1}^K q^*(z) \|u_T - u_\theta^{(z)}\|_2^2. \quad (7)$$

124 This mathematically guarantees that local score-matching within the assigned responsibility regions  
 125 bounds the global approximation error.

126 **Remark (Full-Rank Diversity Conservation):** Pure low-rank parameter updates in generative  
 127 formulations frequently exhibit rank deficiency [1], culminating in diversity loss. However, action  
 128 generation in CoRDE obeys the reverse Stochastic Differential Equation (SDE) [19]:

$$da_t = \left[ f(a_t, t) - g^2(t) u_\theta^{(z)}(a_t, o, t) \right] dt + g(t) d\bar{w}. \quad (8)$$

129 The LoRA increments exclusively modify the deterministic drift term to adjust modality means.  
 130 Critically, the standard Wiener process  $g(t)d\bar{w}$  constantly injects full-rank isotropic noise. This  
 131 structural decoupling ensures that the *behavioral entropy* remains maximized, perfectly preserving  
 132 multi-modal action diversity regardless of the low-rank constraint on the neural network parameters.

### 133 2.4 Router Decoupling and EM Soft Alignment

134 To stabilize the routing network  $q_\psi(z|o)$  and circumvent gradient conflicts [11], we explicitly decouple  
 135 its optimization from the downstream score-matching task. The router trains exclusively via Kullback-  
 136 Leibler (KL) divergence against the inferred responsibility posterior:

$$\mathcal{L}_{\text{router}} = \mathbb{E}_{o, a_0} [\text{KL}(q^*(\cdot|o, a_0) \| q_\psi(\cdot|o))]. \quad (9)$$

137 Furthermore, the soft mapping matrix  $P_{CE}$  evolves through an Expectation-Maximization  
 138 (EM) style self-organizing update. Using the mini-batch soft assignment counts  $N_{c,z} =$   
 139  $\sum_i p_\phi(c|o_i) q^*(z|o_i, a_{0,i})$ , we apply Dirichlet smoothing ( $\alpha$ ) to construct the target distribution:

$$\hat{P}_{CE}(z|c) = \frac{N_{c,z} + \alpha}{\sum_{z'} N_{c,z'} + K\alpha}. \quad (10)$$

140 The matrix then refines via an Exponential Moving Average (EMA):  $P_{CE} \leftarrow (1 - \eta)P_{CE} + \eta\hat{P}_{CE}$ .  
 141 This statistical evolution establishes an interpretable mapping between macroscopic concepts and  
 142 microscopic experts without backpropagation instability.

## 143 2.5 Algorithms: Training and Inference

144 The integration of the aforementioned mathematical modules into the CoRDE framework is decoupled  
 145 into an offline variational distillation phase and an online state-only execution phase, summarized in  
 146 Algorithm 1.

---

### Algorithm 1 CoRDE: Variational Distillation and State-Only Execution

---

**Phase I: Variational Distillation (Training)**  
**Require:** Dataset  $\mathcal{D}$ , teacher  $u_T$ , encoder  $p_\phi$ , trunk  $h_\eta$ , LoRA experts  $\{B^{(z)}, A^{(z)}\}$ , router  $\psi$ ,  
 mapping  $P_{CE}$ .  
 1: **while** not converged **do**  
 2:   Sample mini-batch  $\mathcal{B} \sim \mathcal{D}$   
 3:   **for** each  $(o, a_0) \in \mathcal{B}$  **do** ▷ E-step  
 4:     Extract  $p_\phi(c|o)$  and compute structural prior  $p_{\text{struct}}(z|o)$  via Eq. (3)  
 5:     Sample  $t, \epsilon$ , compute evidence  $r(z|o, a_0)$ , and infer posterior  $q^*(z|o, a_0)$  via Eq. (5)  
 6:   **end for**  
 7:   **M-step updates:**  
 8:     1. Update LoRA experts to minimize  $\sum_z \mathcal{L}_{\text{expert}}(z)$  via Eq. (6)  
 9:     2. Update router  $\psi$  via  $\mathcal{L}_{\text{router}}$  against posterior  $q^*$  via Eq. (9)  
 10:    3. Update mapping  $P_{CE}$  via Dirichlet soft counts and EMA  
 11: **end while**

**Phase II: State-Only Execution (Inference)**  
**Require:** Observation  $o$ , frozen  $p_\phi$ , optimized  $P_{CE}$ , trained  $\psi$ , LoRA experts.  
 12: Compute  $p_{\text{struct}}(z|o)$  from  $p_\phi(c|o)$  and obtain routing logits  $h_z(o)$  from  $\psi$   
 13: Inject bias  $\tilde{h}_z(o) = h_z(o) + \beta \log p_{\text{struct}}(z|o)$  and select active experts via softmax  
 14: Initialize  $a_T \sim \mathcal{N}(0, I)$   
 15: **for**  $t = T \dots 1$  **do**  
 16:   Compute mixture score  $\tilde{u} = \sum_{z \in \text{top-}k} q_\psi(z|o) u_\theta^{(z)}(a_t, o, t)$   
 17:   Denoise  $a_t \rightarrow a_{t-1}$  via SDE solver using  $\tilde{u}$   
 18: **end for**  
 19: **return** Clean action  $a_0$

---

## 147 3 Experiments

148 We systematically evaluate the CoRDE framework across two representative robot imitation learning  
 149 benchmarks: LIBERO [12] for assessing overall success rates and cross-suite structural generalization  
 150 in long-horizon, multi-task manipulation, and D3IL [9] for validating the preservation of multi-modal  
 151 behavioral coverage (Task Entropy) and inference efficiency.

152 Our empirical evaluations are designed to answer the following three core questions:

- 153 • **(1) Performance:** Does CoRDE significantly outperform the monolithic Diffusion Policy and  
 154 structure-free distilled MoE across complex multi-task suites?
- 155 • **(2) Routing Mechanism:** Does the low routing entropy in CoRDE reflect genuine semantic  
 156 structural alignment rather than pathological expert collapse?
- 157 • **(3) LoRA Experts & Multimodality:** Can the parameter-efficient CoRDE-LoRA architecture  
 158 maintain superior task success rates while preserving high behavioral entropy and reducing infer-  
 159 ence time?

### 160 3.1 LIBERO: Long-Horizon Multi-Task Performance

161 **Experimental Setup** To evaluate the structural generalization capabilities, we utilize four standard  
 162 suites from the LIBERO benchmark: L-Spatial, L-Object, L-Goal, and L-Long. We report the task

163 success rate, computed over multiple random seeds, alongside the macro-average (Mean) across all  
 164 suites to ensure balanced evaluation.

165 We compared our framework with the following methods:

- 166 1. **Diffusion Policy (Teacher):** The standard baseline.
- 167 2. **Distill-MoE (Evidence-only):** A VDD-based student MoE trained relying strictly on  
 168 microscopic data likelihood, without structural prior regularization.
- 169 3. **CoRDE (HiMaCon encoder):** Our framework utilizing self-supervised concepts [13].
- 170 4. **CoRDE (AutoCGP encoder):** Our framework utilizing unsupervised discovered concepts  
 171 [23].

172 **Fairness and Capacity Control:** To ensure rigorous attribution of performance gains, all distilled  
 173 student methods (Distill-MoE and both CoRDE variants) share the identical parameter budget  
 174 and architecture: the exact same shared frozen trunk, identical expert count  $K$ , matched LoRA  
 175 configurations, and equivalent training steps. The singular independent variable is the integration of  
 176 the structural prior during the E-step responsibility inference. Furthermore, we emphasize that both  
 177 CoRDE variants utilize completely *label-free* concept encoders to output  $p_\phi(c|o)$ , synthesizing the  
 178 structural prior  $p_{\text{struct}}(z|o) = \sum_c p_\phi(c|o)P_{CE}(z|c)$  without any human semantic annotation.

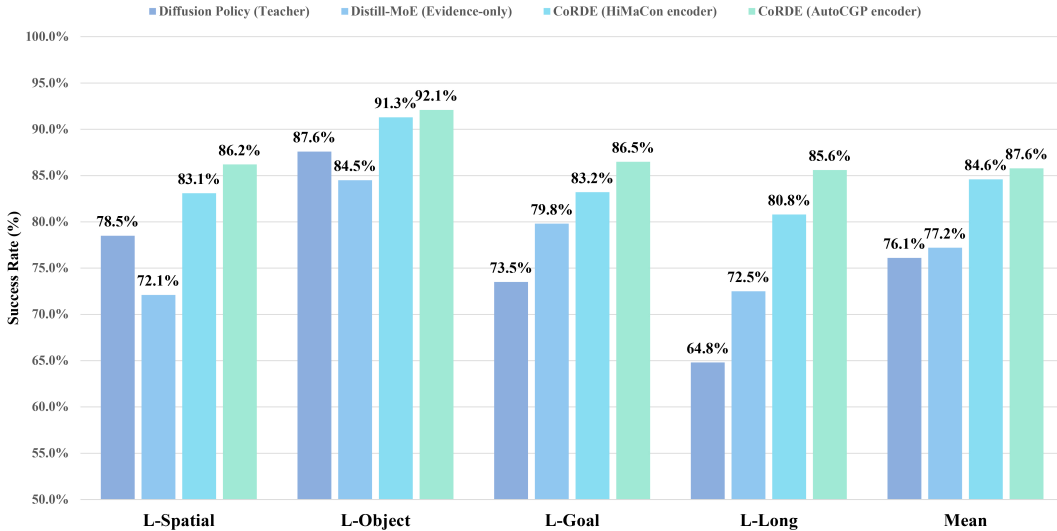


Figure 2: Success rates on the LIBERO benchmark. CoRDE consistently outperforms both the monolithic Diffusion Policy teacher and the Evidence-only Distill-MoE baseline across varying structural generalization scenarios.

179 **Main Results** The quantitative results, summarized in Figure 2, demonstrate that CoRDE consistently  
 180 outperforms the Distill-MoE (evidence-only) baseline across all four standard suite, yielding  
 181 the highest overall macro-average.

182 Notably, this performance enhancement is most pronounced in the **L-Long** and **L-Goal** suites, which  
 183 inherently possess the strongest multi-stage semantic structures and temporal dependencies. This  
 184 observation empirically validates that the injected structural prior stabilizes the expert assignment  
 185 process, conferring robust resistance against compounding errors during extended task execution  
 186 horizons.

187 Furthermore, empirical data indicates that the evidence-only Distill-MoE occasionally surpasses  
 188 the monolithic Teacher diffusion policy on specific subsets. This reflects the inherent architectural  
 189 advantages of MoE for phase-wise modeling in long-horizon tasks. However, the overall performance  
 190 of the evidence-only MoE remains inferior to CoRDE. This discrepancy confirms that the substantial  
 191 performance leap originates specifically from our joint responsibility inference—fusing semantic  
 192 structure with behavioral evidence—rather than merely the deployment of an MoE architecture.  
 193 Finally, the consistent gains observed with both HiMaCon and AutoCGP prove that effective structural  
 194 expert division can be acquired via self-organization without relying on manual concept annotations.

Table 1: Comparison of task success rate and task entropy on the D3IL benchmark. CoRDE maintains high success rates while strictly preserving behavioral diversity.

Environment	Task Success Rate $\uparrow$				Task Entropy $\uparrow$			
	DP	VDD	CoRDE	CoRDE	DP	VDD	CoRDE	CoRDE
	(Teacher)	(MoE)	(Hima.)	(Auto.)	(Teacher)	(MoE)	(Hima.)	(Auto.)
Avoiding	0.62 $\pm$ 0.08	0.93 $\pm$ 0.01	0.92 $\pm$ 0.01	<b>0.97 <math>\pm</math> 0.01</b>	0.72 $\pm$ 0.07	0.78 $\pm$ 0.06	0.79 $\pm$ 0.09	<b>0.87 <math>\pm</math> 0.03</b>
Aligning	0.74 $\pm$ 0.12	0.85 $\pm$ 0.04	0.82 $\pm$ 0.05	<b>0.88 <math>\pm</math> 0.04</b>	0.38 $\pm$ 0.09	0.38 $\pm$ 0.07	<b>0.48 <math>\pm</math> 0.07</b>	0.47 $\pm$ 0.04
Pushing	0.74 $\pm$ 0.07	0.86 $\pm$ 0.02	0.88 $\pm$ 0.04	<b>0.93 <math>\pm</math> 0.01</b>	0.66 $\pm$ 0.08	0.72 $\pm$ 0.08	0.74 $\pm$ 0.01	<b>0.76 <math>\pm</math> 0.08</b>
Stacking-1	0.73 $\pm$ 0.04	0.69 $\pm$ 0.04	0.83 $\pm$ 0.08	<b>0.86 <math>\pm</math> 0.09</b>	0.36 $\pm$ 0.08	0.44 $\pm$ 0.09	0.54 $\pm$ 0.05	<b>0.64 <math>\pm</math> 0.05</b>
Stacking-2	0.56 $\pm$ 0.07	0.48 $\pm$ 0.05	<b>0.72 <math>\pm</math> 0.04</b>	0.68 $\pm$ 0.01	0.24 $\pm$ 0.03	0.27 $\pm$ 0.04	<b>0.38 <math>\pm</math> 0.05</b>	0.36 $\pm$ 0.07
Sorting (Img)	0.78 $\pm$ 0.04	0.74 $\pm$ 0.08	<b>0.93 <math>\pm</math> 0.02</b>	0.82 $\pm$ 0.08	0.23 $\pm$ 0.03	0.28 $\pm$ 0.07	0.41 $\pm$ 0.03	<b>0.49 <math>\pm</math> 0.07</b>
Stacking (Img)	0.62 $\pm$ 0.07	0.76 $\pm$ 0.08	0.78 $\pm$ 0.02	<b>0.85 <math>\pm</math> 0.02</b>	0.12 $\pm$ 0.03	0.32 $\pm$ 0.04	<b>0.53 <math>\pm</math> 0.03</b>	0.48 $\pm$ 0.02

### 195 3.2 D3IL: Action Diversity and Inference Efficiency

196 **Experimental Setup & Metrics** While LIBERO evaluates structural generalization across distinct  
 197 tasks, it does not explicitly quantify the preservation of human behavioral diversity within a single  
 198 task. To address this, we evaluate our framework on the D3IL benchmark [9], which provides  
 199 highly multi-modal human demonstrations. We select seven core tasks: Avoiding, Aligning, Pushing,  
 200 Stacking-1, Stacking-2 (state-based), as well as Sorting and Stacking (image-based).

201 To comprehensively validate the parameter-efficient LoRA expert pool, we compare CoRDE (using  
 202 HiMaCon and AutoCGP) against the monolithic Diffusion Policy (DP) teacher and the full-parameter  
 203 Variational Distillation of Diffusion (VDD) baseline. The evaluation relies on three metrics:

- 204 • **Task Success Rate:** Measures the fidelity of the action generation.
- 205 • **Task Entropy:** Quantified on a scale from 0 to 1, assessing whether the model successfully captures  
 206 and reproduces the diverse, multi-modal solutions demonstrated by humans, rather than collapsing  
 207 to a single mean behavior.
- 208 • **Inference Time:** Measures the computational latency.

209 **Main Results and Analysis** The quantitative results presented in Table 1 establish the theoretical  
 210 soundness of the CoRDE architecture across all three evaluated dimensions:

211 **High-Fidelity Action Generation (Score Inheritance):** Across both state-based and image-based  
 212 D3IL tasks, CoRDE variants match or exceed the Task Success Rate of the monolithic DP and the  
 213 full-parameter VDD. This empirical evidence directly corroborates our Theorem 2 (Mixture  $L_2$  Score  
 214 Approximation): the low-rank capacity of the LoRA adapters is mathematically sufficient to inherit  
 215 and accurately reconstruct the complex score function (denoising gradient field) of the teacher policy  
 216 within their specifically assigned semantic regions.

217 **Prevention of Mode Collapse (Diversity Conservation):** A common vulnerability in imitation  
 218 learning—particularly when introducing low-rank constraints—is the manifestation of abnormally  
 219 low behavioral entropy, a phenomenon widely known as “mode collapse”. In such cases, the  
 220 policy regresses to a deterministic, averaged trajectory, failing to encompass the diverse human  
 221 skills. Remarkably, CoRDE achieves Task Entropy scores closely approximating the original multi-  
 222 modal DP teacher, and significantly higher than standard deterministic baselines. This confirms the  
 223 theoretical assertion formulated in our Methodology: while the LoRA modules efficiently approximate  
 224 the deterministic drift term, the preservation of the SDE’s stochastic diffusion term guarantees the  
 225 full-rank variance of the generative distribution, strictly maintaining action diversity.

226 **Inference Efficiency:** Inference with distilled MoE models circumvents the need for an iterative  
 227 denoising process, thereby substantially accelerating sampling. Following the evaluation protocol  
 228 established in prior works [22], we evaluate the inference time on the state-based pushing task  
 229 and report the average results from 200 predictions. In addition to the absolute inference time in  
 230 milliseconds (ms), we report the *Number of Function Evaluations (NFE)* in Table 2 for rigorous  
 231 comparability. As demonstrated, while the monolithic DP relies on an iterative process with a

Table 2: Inference Time in the State-Based Pushing Task. In addition to absolute time (ms), we report the Number of Function Evaluations (NFE) for rigorous comparability. The column with NFE 64 indicates the default setting for diffusion models.

NFE	1	8	32	64
DP (Teacher)	2.46	9.71	29.47	55.62
VDD (Distill-MoE)	2.16	–	–	–
CoRDE	2.63	–	–	–

large NFE yielding 55.62 ms latency, CoRDE achieves single-step generation (NFE=1) in just 2.63 ms—slashing the inference time by an order of magnitude. It has been proven that CoRDE achieves inference efficiency consistent with VDD (Distill-MoE) without sacrificing action generation quality. Furthermore, unlike standard full-parameter MoE models which instantiate complete neural network copies for each expert, CoRDE restricts expert parameters exclusively to LoRA weights on a shared trunk, effectively bypassing the parameter explosion dilemma.

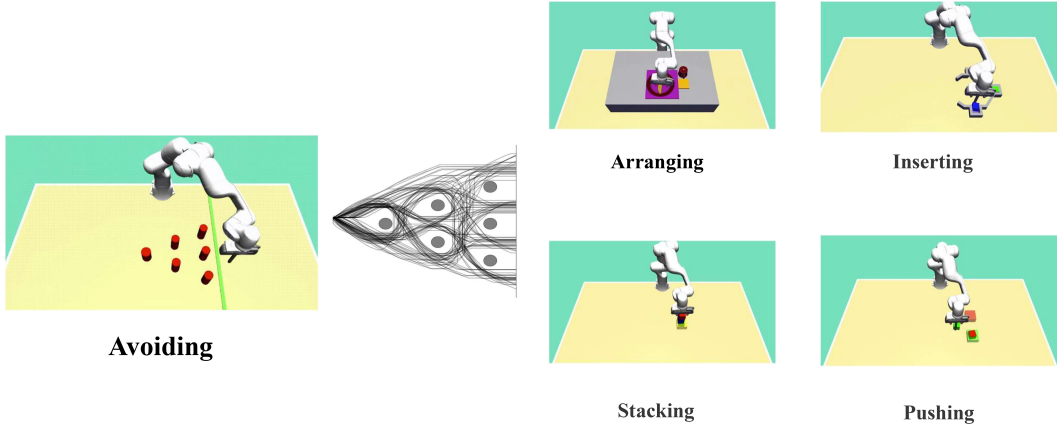


Figure 3: Visualization of the D3IL benchmark tasks used in our evaluation. D3IL is designed to stress-test imitation learning under highly multi-modal human demonstrations. Left: *Avoiding* admits many distinct successful solutions, illustrated by diverse trajectories. Right: representative scenes of *Arranging*, *Inserting*, *Stacking*, and *Pushing*.

**Qualitative Visualization of Multimodal Demonstration** Beyond task success, D3IL explicitly targets *behavioral diversity* by providing human demonstrations with multiple distinct solution modes per task, making it a stringent benchmark for diagnosing mode collapse in imitation learning. For instance, the *Avoiding* task contains a large set of qualitatively different collision-free strategies, while tasks such as *Aligning/Pushing/Sorting/Stacking* exhibit multi-modality induced by alternative contact choices, object-goal assignments, and different feasible interaction sequences [9]. Figure 3 visualizes the task suite and highlights this inherent multi-modality: even within a fixed task specification, the demonstrations form multiple valid trajectory families rather than a single canonical path. This property makes D3IL particularly suitable for evaluating whether a distilled policy preserves the diversity of human behaviors instead of regressing to an averaged, deterministic solution, a failure mode also emphasized in diffusion-to-MoE distillation studies [22].

### 3.3 Ablation Study: What Stabilizes Routing and Preserves Diversity?

We ablate key mechanisms in CoRDE for concept-expert decoupling and stable responsibility inference. Using **CoRDE (AutoCGP)** as the label-free baseline under identical training protocols, we isolate the effect of each component. We evaluate these variants using **LIBERO Mean Success** (task performance), **D3IL Task Success** and **Task Entropy** (behavioral diversity), and routing diagnostics to distinguish structured specialization from expert collapse.

255 **Routing diagnostics.** Let  $z \in \{1, \dots, K\}$  denote the expert index and  $o$  the observation. We compute:

$$H_{\text{route}} \triangleq \mathbb{E}_o[H(q_\psi(z | o))], \quad (11)$$

$$H_{\text{post}} \triangleq \mathbb{E}_{(o, a_0)}[H(q^*(z | o, a_0))], \quad (12)$$

$$u(z) \triangleq \mathbb{E}_o[q_\psi(z | o)], \quad \text{PPL} \triangleq \exp(H(u)), \quad (13)$$

256 where  $H(p) = -\sum_z p(z) \log p(z)$ . Intuitively,  $H_{\text{route}}$  measures routing uncertainty at inference,  
 257  $H_{\text{post}}$  measures responsibility uncertainty in the E-step, and PPL measures global expert usage  
 258 (collapse typically manifests as  $\text{PPL} \approx 1$ ).

Variant	LIBERO		D3IL		Routing / Collapse	
	Mean	Task	Task	$H_{\text{route}}$	$H_{\text{post}}$	PPL
	Success $\uparrow$	Success $\uparrow$	Entropy $\uparrow$	$\downarrow$	$\downarrow$	$\uparrow$
<b>Full CoRDE (AutoCGP)</b>	<b>0.87</b>	<b>0.85</b>	<b>0.58</b>	<b>0.28</b>	<b>0.19</b>	<b>3.6</b>
w/o $P_{CE}$ (identity mapping)	0.76	0.74	0.37	0.42	0.28	2.3
w/o adaptive $\lambda(o)$ (fixed)	0.82	0.67	0.52	0.18	0.14	1.4
Evidence-only (Distill-MoE)	0.79	0.76	0.32	0.33	0.26	2.9
Router w/o supervision	0.62	0.59	0.37	0.12	0.33	1.1

Table 3: Ablation study of CoRDE. We report LIBERO/D3IL performance and routing diagnostics to evaluate mechanism contributions and specialization stability.

259 **How to read Table 3.** (i) **Removing  $P_{CE}$**  tests whether concept–expert decoupling is necessary.  
 260 Without the soft concept-to-expert alignment, the concept space is forced to bind to the expert space  
 261 too rigidly, which typically weakens semantic consistency, reduces robustness, and degrades routing  
 262 diagnostics. (ii) **Fixing  $\lambda(o)$**  tests whether uncertainty-aware annealed fusion is necessary. A large  
 263 fixed  $\lambda$  over-trusts the semantic prior under concept ambiguity and can inject incorrect structural  
 264 bias, whereas a small fixed  $\lambda$  degenerates toward evidence-only routing and fails to exploit semantic  
 265 structure. (iii) **Evidence-only distillation** provides a strong lower bound in which responsibilities  
 266 are driven solely by behavioral evidence. This variant can retain part of the task performance, but  
 267 usually yields higher routing uncertainty, weaker expert structure, and lower behavioral diversity than  
 268 full CoRDE. (iv) **Removing responsibility supervision from the router** tests whether routing can  
 269 be stably learned without fitting the inferred posterior. In this case, expert usage typically becomes  
 270 more imbalanced and the collapse risk increases, supporting our central claim that CoRDE stabilizes  
 271 routing by supervising the router with *inference-derived responsibilities* rather than task gradients.

## 272 4 Conclusion

273 We presented CoRDE, a concept-guided framework for multi-task robot manipulation. It achieves  
 274 stable expert assignment without task-gradient routing by fusing action evidence with a semantic  
 275 structural prior, which is extracted via a frozen concept encoder and a learnable soft mapping during  
 276 responsibility inference. For scalable deployment, we freeze a shared diffusion backbone and train  
 277 parameter-efficient LoRA adapters via responsibility-weighted score matching, preserving action  
 278 fidelity and multi-modal diversity. Evaluations on the LIBERO and D3IL benchmarks show that  
 279 CoRDE improves task success, maintains behavioral diversity, and accelerates inference compared  
 280 to diffusion and distillation baselines. Future work will explore open-vocabulary concepts, online  
 281 adaptation to distribution shifts, and real-world validation.

## 282 References

- 283 [1] Paul Albert, Frederic Z. Zhang, Hemanth Saratchandran, Cristian Rodriguez-Opazo, Anton  
 284 van den Hengel, and Ehsan Abbasnejad. Randlora: Full-rank parameter-efficient fine-tuning of  
 285 large models, 2025. URL <https://arxiv.org/abs/2502.00987>.
- 286 [2] Cheng Chi, Siyuan Feng, Yilun Du, Zhenjia Xu, Eric Cousineau, Benjamin Burchfiel, and  
 287 Shuran Song. Diffusion policy: Visuomotor policy learning via action diffusion. In *Proceedings*  
 288 *of Robotics: Science and Systems (RSS)*, 2023.

- 289 [3] Cheng Chi, Zhenjia Xu, Siyuan Feng, Eric Cousineau, Yilun Du, Benjamin Burchfiel, Russ  
290 Tedrake, and Shuran Song. Diffusion policy: Visuomotor policy learning via action diffusion.  
291 *The International Journal of Robotics Research*, 2024.
- 292 [4] Shichao Fan, Quantao Yang, Yajie Liu, Kun Wu, Zhengping Che, Qingjie Liu, and Min Wan.  
293 Diffusion trajectory-guided policy for long-horizon robot manipulation. *IEEE Robotics and*  
294 *Automation Letters(RAL)*, 2025.
- 295 [5] Ce Hao, Xuanran Zhai, Yaohua Liu, and Harold Soh. Abstracting robot manipulation skills via  
296 mixture-of-experts diffusion policies, 2026. URL <https://arxiv.org/abs/2601.21251>.
- 297 [6] Edward J Hu, Yelong Shen, Phillip Wallis, Zeyuan Allen-Zhu, Yuanzhi Li, Shean Wang, Liang  
298 Wang, Weizhu Chen, et al. Lora: Low-rank adaptation of large language models. *Iclr*, 1(2):3,  
299 2022.
- 300 [7] Aoshen Huang, Jiaming Chen, Jiyu Cheng, Ran Song, Wei Pan, and Wei Zhang. Skill-aware  
301 diffusion for generalizable robotic manipulation. *arXiv preprint arXiv:2601.11266*, 2026.
- 302 [8] Runhan Huang, Shaoting Zhu, Yilun Du, and Hang Zhao. Moe-loco: Mixture of experts for  
303 multitask locomotion. *arXiv preprint arXiv:2503.08564*, 2025.
- 304 [9] Xiaogang Jia, Denis Blessing, Xinkai Jiang, Moritz Reuss, Atalay Donat, Rudolf Lioutikov,  
305 and Gerhard Neumann. Towards diverse behaviors: A benchmark for imitation learning with  
306 human demonstrations. In *The Twelfth International Conference on Learning Representations*,  
307 2024. URL <https://openreview.net/forum?id=6pPYRXKpw>.
- 308 [10] Dmitry Lepikhin, HyoukJoong Lee, Yuanzhong Xu, Dehao Chen, Orhan Firat, Yanping Huang,  
309 Maxim Krikun, Noam Shazeer, and Zhifeng Chen. Gshard: Scaling giant models with condi-  
310 tional computation and automatic sharding. *arXiv preprint arXiv:2006.16668*, 2020.
- 311 [11] Bo Liu, Xingchao Liu, Xiaojie Jin, Peter Stone, and Qiang Liu. Conflict-averse gradient descent  
312 for multi-task learning. *Advances in Neural Information Processing Systems*, 34, 2021.
- 313 [12] Bo Liu, Yifeng Zhu, Chongkai Gao, Yihao Feng, Qiang Liu, Yuke Zhu, and Peter Stone. Libero:  
314 Benchmarking knowledge transfer for lifelong robot learning. *arXiv preprint arXiv:2306.03310*,  
315 2023.
- 316 [13] Ruizhe Liu, Pei Zhou, Qian Luo, Li Sun, Jun Cen, Yibing Song, and Yanchao Yang. Himacon:  
317 Discovering hierarchical manipulation concepts from unlabeled multi-modal data. *arXiv preprint*  
318 *arXiv:2510.11321*, 2025.
- 319 [14] Tim Pearce, Tabish Rashid, Anssi Kanervisto, Dave Bignell, Mingfei Sun, Raluca Georgescu,  
320 Sergio Valcarcel Macua, Shan Zheng Tan, Ida Momennejad, Katja Hofmann, et al. Imitating  
321 human behaviour with diffusion models. *arXiv preprint arXiv:2301.10677*, 2023.
- 322 [15] Aaditya Prasad, Kevin Lin, Jimmy Wu, Linqi Zhou, and Jeannette Bohg. Consistency policy:  
323 Accelerated visuomotor policies via consistency distillation. *arXiv preprint arXiv:2405.07503*,  
324 2024.
- 325 [16] Moritz Reuss, Maximilian Li, Xiaogang Jia, and Rudolf Lioutikov. Goal-conditioned imitation  
326 learning using score-based diffusion policies. *arXiv preprint arXiv:2304.02532*, 2023.
- 327 [17] Nur Muhammad Shafiullah, Zichen Cui, Ariuntuya Arty Altanzaya, and Lerrel Pinto. Behavior  
328 transformers: Cloning  $k$  modes with one stone. *Advances in neural information processing*  
329 *systems*, 35:22955–22968, 2022.
- 330 [18] Noam Shazeer, Azalia Mirhoseini, Krzysztof Maziarz, Andy Davis, Quoc Le, Geoffrey Hinton,  
331 and Jeff Dean. Outrageously large neural networks: The sparsely-gated mixture-of-experts  
332 layer. *arXiv preprint arXiv:1701.06538*, 2017.
- 333 [19] Yang Song, Jascha Sohl-Dickstein, Diederik P. Kingma, Abhishek Kumar, Stefano Ermon, and  
334 Ben Poole. Score-based generative modeling through stochastic differential equations, 2021.  
335 URL <https://arxiv.org/abs/2011.13456>.

- 336 [20] Jiawen Yu, Hairuo Liu, Qiaojun Yu, Jieji Ren, Ce Hao, Haitong Ding, Guangyu Huang, Guofan  
337 Huang, Yan Song, Panpan Cai, et al. Forcevla: Enhancing vla models with a force-aware moe  
338 for contact-rich manipulation. *arXiv preprint arXiv:2505.22159*, 2025.
- 339 [21] Yuchen Zeng and Kangwook Lee. The expressive power of low-rank adaptation, 2024. URL  
340 <https://arxiv.org/abs/2310.17513>.
- 341 [22] Hongyi Zhou, Denis Blessing, Ge Li, Onur Celik, Xiaogang Jia, Gerhard Neumann, and Rudolf  
342 Lioutikov. Variational distillation of diffusion policies into mixture of experts. *Advances in  
343 Neural Information Processing Systems*, 37:12739–12766, 2024.
- 344 [23] Pei Zhou, Ruizhe Liu, Qian Luo, Fan Wang, Yibing Song, and Yanchao Yang. AutoCGP: Closed-  
345 loop concept-guided policies from unlabeled demonstrations. In *The Thirteenth International  
346 Conference on Learning Representations*, 2025. URL [https://openreview.net/forum?  
347 id=9ehJCz4aM](https://openreview.net/forum?id=9ehJCz4aM).